An MC-SCF Study of Styrene Singlet-State Photoisomerization

Michael J. Bearpark,† Massimo Olivucci,*,‡ Sarah Wilsey,† Fernando Bernardi,‡ and Michael A. Robb*,†

Contribution from the Dipartimento di Chimica "G. Ciamician" dell'Università di Bologna, Via Selmi 2, 40126 Bologna, Italy, and Department of Chemistry, King's College, London, Strand, London WC2R 2LS, U.K.

Received November 7, 1994[⊗]

Abstract: The decay processes involved in the photochemical double bond isomerization of styrene are documented by means of MC-SCF computations. Possible intersystem crossing (ISC) and internal conversion (IC) pathways have been studied by geometry optimization of the lowest points on the potential energy surface crossings and computation of the spin−orbit coupling constants. The isomerization of β-methylstyrene (1-phenylpropene) proceeds (Lewis, F. D.; Bassani, D. M. *J. Am. Chem. Soc.* **1993**, *115*, 7523−7524) via temperature-independent and temperature-dependent pathways in solution. The temperature-independent isomerization process is consistent with a reaction path that begins with ISC at an S_1/T_2 crossing which occurs at the planar S_1 minimum. The lowest-energy S_1/S_0 crossing minimum (conical intersection) is benzene-like, and will not lead to isomerization. Rather, the second temperature-dependent isomerization mechanism also begins with ISC either at the twisted S_1 minimum (also an S_1/T_2 crossing) or at the planar S_1 minimum *after* adiabatic *cis−trans* isomerization on S_1 has occurred. Decay from T_2 to S_0 takes place via a T_2/T_1 conical intersection, followed by one of two different T_1/S_0 crossing points: the expected twisted T_1 minimum, or a higher-energy benzene-like structure. Because of the large energy gap, $S_1 \rightarrow S_0$ IC at the twisted S_1 minimum is unlikely to take place as previously suggested.

Introduction

The photochemistry of aryl olefin double bond isomerization has been the subject of complementary experimental and theoretical research for several decades.[1] Modern time-resolved experimental methods have made detailed kinetic and energetic information available. However, in the case of the simplest aryl olefin—styrene (**1**)—the most recent theoretical studies are almost ten years old[2−7] and are not sufficient to rationalize current experimental observations.[8] Our objective is to document possible intersystem crossing (ISC) and internal conversion (IC) pathways by full geometry optimization of the lowest energy points on the potential surface crossings and to compute the spin−orbit coupling constants where appropriate.

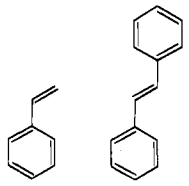

1 2

The accepted mechanism[1,9] for the S_1 photochemical isomerization of aryl olefins such as styrene and stilbene (**2**) is based on ethylene: the decay funnel is a twisted minimum on S_1 which is almost coincident with a transition structure on S_0. The barrier to twisting on S_1 is due to an avoided crossing with a doubly-excited state (not present in ethylene) in which the olefin bond is effectively reduced to a single bond. However, there are differences in the photophysics of styrene and stilbene which cannot be explained by such a model. Decay from S_1 *trans*-stilbene occurs within tens to hundreds of picoseconds, and is friction dependent. Similarly, decay in *cis*-stilbene takes place within 0.3−2 ps, even in viscous media.[1,10] For styrene, however, Condirston and Laposa[11a] have measured a much longer S_1 lifetime of 14.6 ns at 298 K using 3-methylpentane as a solvent. They also obtained a value of 0.24 for the fluorescence quantum yield of styrene under the same conditions,[12] whereas the corresponding value for *cis*-stilbene is much smaller ($\sim 8 \times 10^{-5}$).[13] Condirston and Laposa found that non-radiative decay pathways were still operating in styrene at 77 K: the fluorescence quantum yield was 0.46 at this temperature,[11a] whereas for *trans*-stilbene this value is ~1.0.[11b] ISC in stilbene is negligible.[1] However, for styrene, the ISC quantum yield measured by Bonneau[14] is 0.4, which implies that spin-forbidden processes may be competitive with IC and fluorescence.

From a conceptual point of view, it is essential to understand the role of the aromatic ring system which is coupled to the

† King's College.

‡ Dipartimento di Chimica "G. Ciamician" dell'Università di Bologna.

[⊗] Abstract published in *Advance ACS Abstracts*, June 15, 1995.

(1) (a) Saltiel, J.; Sun, Y.-P. In *Photochromism: Molecules and Systems*; Dürr, H., Bouas-Laurent, H., Eds.; Elsevier: Amsterdam, 1990; pp 64 and references cited therein. (b) Saltiel, J.; Waller, S. A.; Sears, D. F. *Photochem. Photobiol.* **1992**, *65*, 29.

(2) Hemley, R. J.; Dinur, U.; Vaida, V.; Karplus, M. *J. Am. Chem. Soc.* **1985**, *107*, 836.

(3) Said, M.; Malrieu, J. P. *Chem. Phys. Lett.* **1983**, *102*, 312.

(4) Nebot-Gil, I.; Malrieu, J. P. *Chem. Phys. Lett.* **1981**, *84*, 571.

(5) Orlandi, G.; Palmieri, P.; Poggi, G. *J. Chem. Soc., Faraday Trans. 2* **1981**, *77*, 71.

(6) Bendazzoli, G. L.; Orlandi, G.; Palmieri, P.; Poggi, G. *J. Am. Chem. Soc.* **1978**, *100*, 392.

(7) Bruni, M. C.; Momicchioli, F.; Baraldi, I.; Langlet, J. *Chem. Phys. Lett.* **1975**, *36*, 484.

(8) (a) Lewis, F. D.; Bassani, D. M. *J. Am. Chem. Soc.* **1993**, *115*, 7523. (b) Lewis, F. D.; Bassani, D. M.; Caldwell, R. A.; Unett, D. J. *J. Am. Chem. Soc.* **1994**, *116*, 10477.

(9) Orlandi, G.; Siebrand, W. *Chem. Phys. Lett.* **1975**, *30*, 352.

(10) Sension, R. J.; Repinec, S. T.; Szarka, A. Z.; Hochstrasser, R. M. *J. Chem. Phys.* **1993**, *98*, 6291 and references cited therein.

(11) (a) Condirston, D. A.; Laposa, J. D. *Chem. Phys. Lett.* **1979**, *63*, 313. (b) Sumitani, M.; Nakashima, N.; Yoshihara, K.; Nagakura, S. *Chem. Phys. Lett.* **1977**, *51*, 183.

(12) Lyons and Turro (Lyons, A. L.; Turro, N. J. *J. Am. Chem. Soc.* **1978**, *100*, 3177) measured the styrene S_1 lifetime as 21.7 ns in cyclohexane at 298 K, and a fluorescence quantum yield of 0.22 (relative to 0.15 for biphenyl).

(13) Saltiel, J.; Waller, A. S.; Sears, D. F. *J. Am. Chem. Soc.* **1993**, *115*, 2453.

(14) Bonneau, R. *J. Am. Chem. Soc.* **1982**, *104*, 2921.

0002-7863/95/1517-6944$09.00/0 © 1995 American Chemical Society

double bond. In particular, we are interested in understanding which features of the potential energy surface of styrene arise from the coupling of the ethylene and benzene π-systems and which are associated with the ethylene or benzene ring alone. Using a VB model, the various excited state pathways can be understood in terms of the interplay between "electronic isomers". Presented in a qualitative way in this paper, this model has been derived through the analysis of the MC-SCF wave functions into VB spin coupling patterns.

Recently, the photophysics and photochemistry of styrene have been investigated using several modern experimental techniques. Swiderek,[25] using electron energy loss spectroscopy, gives the order of vertically excited states as $T_1 < T_2 < S_1 < S_2 + S_3$ (the S_2 and S_3 states—one of which is believed to be ionic[2,3]—overlap so strongly that they cannot be distinguished). High-resolution optical spectroscopy[15-17] shows that the equilibrium geometry of the first singlet excited state (S_1) of styrene is planar. Further, the lack of vibrational activity suggests that the $S_0 \rightarrow S_1$ 0–0 transition is almost vertical[19] and similar to the $S_0 \rightarrow S_1$ transition in benzene (which involves uniform ring expansion.[20]) This result disagrees with the earlier work of Hui and Rice,[18] who had suggested that a twisted structure was the overall minimum. Salisbury[23] observed two components in the emission spectrum of S_2. He suggested that rapid IC to vibrationally-excited S_1 could be followed by decay from both twisted and planar S_1 minima,[24] i.e. both exist. Syage and Zewail[16] have identified a barrier of at least 1200 cm^{-1} (3.4 kcal mol^{-1}) to the double bond twisting on S_1.

The S_2 equilibrium structure of styrene is also believed to be planar. The resonance Raman spectrum[21] shows no double bond torsional activity, and the low-frequency progression in the supersonic jet absorption spectrum[22] was assigned[19] to a large-amplitude planar ring distortion in preference to ethylene twisting. By comparing time-resolved photoacoustic calorimetry and oxygen-perturbed absorption measurements, Ni, Caldwell, and Melton[26] assigned the 0–0 $S_0 \rightarrow T_1$ transition to a planar structure, which relaxes to a lower energy minimum by ethylene twisting.

Lewis and Bassani[8] have investigated the photochemistry of 1-phenylpropene (β-methylstyrene) in solution (n-hexane) at different temperatures (220–575 K) using direct irradiation (281 nm) of the lowest energy band. They identify two different ethylene isomerization mechanisms: one temperature independent and one temperature dependent. At low temperatures (i.e. below 290 K in *trans*-1-phenylpropene), they found the rate of isomerization to be temperature independent, indicating that no excited state activation barrier was involved in this process. They further suggest that a triplet state may be involved and the longer excited state lifetime (11.8 ns) may result from a relatively slow ISC step. A triplet route for the styrene isomerization has previously been proposed by other authors. In 1973, Rockley and Salisbury[28] found that the gas-phase isomerization yield of 1-phenylpropene excited throughout the S_1 region was approximately constant, indicating that the rate-limiting step was ISC (a conclusion also reached by Nakagawa and Sigal[29]). Such a route was assumed by Bonneau,[14] and ISC via higher triplet states has also recently been suggested by Swiderek.[25] Since phosphorescence has not been detected despite repeated attempts,[11,12,27] there must be a very efficient decay path from T_2.

The second isomerization mechanism detected by Lewis and Bassani[8] dominates at higher temperatures. This mechanism is associated with the presence of an energy barrier (8.8 kcal mol^{-1} for *trans*-1-phenylpropene and 4.6 kcal mol^{-1} for *cis*-1-phenylpropene) on S_1 which leads to a second radiationless decay channel. In contrast with the temperature-independent process, this relaxation to S_0 was assumed[8] to involve singlet states alone.

At room temperature, the sum of twice the temperature-independent isomerization quantum yield plus the fluorescence quantum yield of 1-phenylpropene is less than unity. This behavior can only be explained by the presence of a radiationless decay channel which leads to regeneration of starting material. This was assigned by Lewis and Bassani[8] to an IC mechanism. A non-photochemical radiationless decay channel appears to open up when styrenes are photoexcited with wavelengths short enough to populate the S_2 state. When S_2 is irradiated, Rockley and Salisbury[28] observed that the isomerization quantum yield falls to zero suggesting a fast IC decay pathway with a large activation barrier on S_1.[30]

The most recent theoretical studies of styrene are those of Hemley et al.,[2] Malrieu et al.,[3,4] and Palmieri et al.[5,6] The S_1 state is predicted to be covalent, but the ionic/covalent character of the S_2/S_3 states has not yet been established. Using a minimal basis and extended CI, Malrieu[4] argues that two ionic states—methyl$^-$benzyl$^+$ and methyl$^+$benzyl$^-$ states—lie between the covalent S_1 and S_2 at the 90° twisted S_0 geometry. This disagrees with the calculations of Bruni et al.,[7] who had suggested that the twisted geometry was the minimum on S_1 and corresponds to the $\pi\pi^*$ (V) state of the ethylene fragment. Bendazzoli et al.,[5] using a diffuse one-electron basis and more limited CI, found the methyl$^+$benzyl$^-$ state and covalent S_1 states to be approximately degenerate at the twisted S_0 geometry. The only previous theoretical studies to use full geometry optimization are those of Said and Malrieu[3] (which was restricted to the covalent states) and Hemley et al.[2] Said and Malrieu confirmed that the S_1 twisted minimum has S_2 character[9] (i.e. correlates with the S_2 excited state of styrene) and found that the optimum angle of twist is about 75°. The barrier height was estimated to be about 17 kcal mol^{-1}, which agrees closely with the energy obtained by Bendazzoli et al.[6] using interpolated geometries. Said and Malrieu also reported that the S_1 and T_2 states were degenerate at this twisted geometry and state that this is the

(15) (a) Hollas, J. M.; Ridley, T. *Chem. Phys. Lett.* **1980**, *75*, 94. (b) Hollas, J. M.; Ridley, T. *J. Mol. Spectrosc.* **1981**, *89*, 232. (c) Hollas, J. M.; Khalilipur, E.; Thakur, S. N. *J. Mol. Spectrosc.* **1978**, *73*, 240.

(16) Syage, J. A.; Al Adel, F.; Zewail, A. H. *Chem. Phys. Lett.* **1983**, *103*, 15.

(17) (a) Seeman, J. I.; Grassian, V. H.; Bernstein, E. R. *J. Am. Chem. Soc.* **1988**, *110*, 8542. (b) Grassian, V. H.; Bernstein, E. R.; Secor, H. V.; Seeman, J. I. *J. Phys. Chem.* **1989**, *93*, 3470.

(18) Hui, M. H.; Rice, S. A. *J. Chem. Phys.* **1974**, *61*, 833.

(19) Hemley, R. J.; Leopold, D. G.; Vaida, V.; Karplus, M. *J. Chem. Phys.* **1985**, *82*, 5379.

(20) Palmer, I. J.; Ragazos, I. N.; Bernardi, F.; Olivucci, M.; Robb, M. A. *J. Chem. Soc.* **1993**, *115* 673.

(21) Zeigler, L. D.; Varotsis, C. *Chem. Phys. Lett.* **1986**, *123*, 175.

(22) Hemley, R. J.; Leopold, D. G.; Vaida, V.; Roebber, J. L. *J. Phys. Chem.* **1981**, *85*, 134.

(23) (a) Steer, R. P.; Swords, M. D.; Crosby, P. M.; Phillips, D.; Salisbury, K. *Chem. Phys. Lett.* **1976**, *43*, 461. (b) Ghiggino, K. P.; Phillips, D.; Salisbury, K.; Swords, M. D. *J. Photochem.* **1977**, *7*, 141. (c) Ghiggino, K. P.; Hara, K.; Salisbury, K.; Philips, D. *J. Photochem.* **1978**, *8*, 267. (d) Ghiggino, K. P.; Hara, K.; Mant, G. R.; Phillips, D.; Salisbury, K.; Steer, R. P.; Swords, M. D. *J. Chem. Soc.*, Perkin *Trans 2* **1978**, 88.

(24) Gustav, K.; Kempka, U.; Suhnel, J. *Theochem. (J. Mol. Struct.)* **1981**, *3*, 181.

(25) Swiderek, P.; Fraser, M.-J.; Michaud, M.; Sanche, L. *J. Chem. Phys.* **1994**, *100*, 70.

(26) Ni, T.; Caldwell, R. A.; Melton, L. A. *J. Am. Chem. Soc.* **1989**, *111*, 457.

(27) Crosby, P. M.; Dyke, J. M.; Metcalfe, J.; Rest, A. J.; Salisbury, K.; Sodeau, J. R. *J. Chem. Soc., Perkin Trans. 2* **1977**, 182.

(28) Rockley, M. G.; Salisbury, K. *J. Chem. Soc., Perkin Trans. 2* **1973**, 1582.

(29) Nakagawa, C. S.; Sigal, P. *J. Chem. Phys.* **1973**, *58*, 3529.

(30) Gas-phase polymerization or radical formation may account for this decrease, as suggested in refs 21 and 28.

de-excitation funnel for isomerization following the standard model.[9] Hemley et al. considered only the singlet states and suggest that the large barrier to adiabatic isomerization must indicate that higher excited singlets are involved in this process.

Computational Details

Our objective in this work is to document possible ISC and IC decay pathways by optimizing the geometry of the lowest energy surface crossing points and computing the spin–orbit coupling constants. An IC process becomes fully efficient at a conical intersection and takes place within the time scale of one vibrational period. In contrast, ISC requires the existence of a singlet–triplet crossing, but the efficiency of the process depends on dynamic effects and the nature of the spin–orbit coupling. Many vibrational periods may be required. Of course, both IC and ISC can occur anywhere on the surface of intersection, not just at the minimum point. However, for small excess energies in condensed phases it is reasonable to assume that decay occurs in the low-energy region of the crossing.

All of the CAS-SCF results presented in this paper have been produced using the MC-SCF program distributed in Gaussian 92.[31] The location of the surface crossings corresponding to conical intersection points and singlet–triplet crossings has been carried out using a non-standard method which we have documented elsewhere[32] and which has been implemented in a development version of Gaussian. Spin–orbit coupling constants have been calculated in an approximation using scaled nuclear charges[33] and one-electron integrals of the H_{LS} operator, implemented in a development version of Gaussian.

In a polyatomic system the "non-crossing rule" (which holds for diatomics) is not valid and two electronic states of the same spatial/spin symmetry may cross at a conical intersection.[34] Conical intersections have been extensively discussed in the literature,[35] and recent CAS-SCF investigations have indicated that they can be a common feature in organic systems.[36] A conical intersection of two potential energy surfaces can be pictured as a "curve" spanning an $(n - 2)$-dimensional subspace of the n nuclear coordinates called the *intersection space*. At any point in this space, the energies of the two states remain the same; the degeneracy is only lifted when the geometry is distorted along the two remaining linearly independent nuclear coordinates x_1 and x_2. These two coordinates are referred to as the *branching space*, and when the energy of the two states is plotted in this space the corresponding potential energy surface looks like a double-cone as depicted in Scheme 1. The vectors x_1 and x_2 are directions defined by the non-adiabatic coupling and gradient difference vectors respectively.[32a,b] If the intersecting potential energy surfaces have different spin multiplicity then x_1 is zero; a singlet–triplet surface crossing occurs along an $(n - 1)$-dimensional intersection space. In this case, the branching space is one-dimensional and corresponds to the gradient difference vector x_2.

Scheme 1

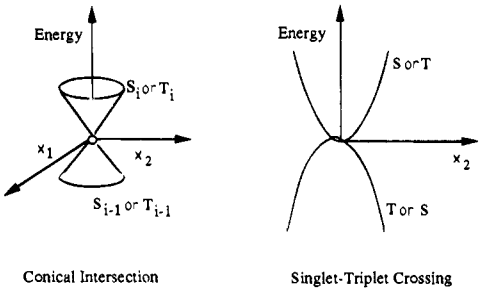

Conical Intersection Singlet-Triplet Crossing

The choice of active space in our computations is unambiguous: the eight electrons and eight orbitals which form the π-system of styrene. The resulting ~2000-term MC-SCF wave function is capable of describing all states that can arise from all possible arrangements of 8 electrons in 8 orbitals. *All the orbitals are fully utilized and optimized* in the computation, but only the active orbitals can have variable occupancy. The identification of 8 p^π active orbitals is merely a specification of which orbitals can have occupancy other than 2. As the geometry is changed from a planar arrangement, the optimization of the orbitals mixes σ/π orbitals to give the lowest energy. The only type of interaction that is not included explicitly at the CI level would result from single excitations of the σ backbone. However, this type of interaction is included through the Brillouin condition satisfied by the optimum MC-SCF orbitals.

Since we have explored the S_1, S_2, T_1, and T_2 surfaces in considerable detail with a large active space, we have restricted ourselves to a modest 4-31G basis set for geometry optimizations. The energetics have then been recomputed with polarization functions (6-31G*). This is adequate to determine the surface topology of the covalent states as we have demonstrated in a previous study of the "channel 3" problem in benzene.[20] In order to describe the ionic states, a basis set containing diffuse functions and an increased active space consisting of both "tight" and "diffuse" p^π orbitals are required, as shown in benzene computations of Roos et al.[37] To improve the description of the ionic state in our calculations, we have added diffuse functions by using the 6-31+G* basis set.

Results and Discussion

(i) A VB Overview of the Relaxation Pathways of Styrene. The covalent excited states of an aryl olefin can be represented in terms of simple VB structures in which the spin coupling of each pair of electrons is identified. (For a theoretical discussion of spin coupling with VB theory, see a standard textbook such as ref 38.) In general, each pair is either singlet coupled (represented by a solid line) or triplet coupled (dashed line). In this section we illustrate the geometric and electronic character of the relaxation/decay pathways which have been located on S_1, S_2, T_1, and T_2. Since we approximate the overall spin coupling in styrene as a superposition of benzene and ethylene

(31) Frisch, M. J.; Trucks, G. W.; Head-Gordon, M.; Gill, P. M. W.; Wong, M. W.; Foresman, J. B.; Schlegel, H. B.; Robb, M. A.; Reploge, E. S.; Gomperts, R.; Andres, J. L.; Raghavachari, K.; Binkley, J. S.; Gonzales, C.; Martin, R. L.; Fox, D. J.; Defrees, D. J.; Baker, J.; Stewart, J. J. P.; Pople, J. A. *Gaussian 92, Revision B*; Gaussian, Inc.: Pittsburgh, 1992.

(32) (a) Ragazos, I. N.; Robb, M. A.; Bernardi, F.; Olivucci, M. *Chem. Phys. Lett.* **1992**, *197*, 217. (b) Bearpark, M. J.; Robb, M. A.; Schlegel, H. B. *Chem. Phys. Lett.* **1994**, *223*, 269.

(33) (a) Langhoff, S.; Kern, C. W. In *Applications of Electronic Structure Theory*; Schaefer, H. F., Ed.; Plenum: New York, 1977; Chapter 10. (b) Yarkony, D. R. *J. Am. Chem. Soc.* **1992**, *114*, 5406. (c) Koseki, S.; Schmidt, M. W.; Gordon, M. S. *J. Phys. Chem.* **1992**, *96*, 10768.

(34) Salem, L. *Electrons in Chemical Reactions: First Principles*; Wiley: New York, 1982.

(35) (a) Von Neumann, J.; Wigner, E. *Phys. Z.* **1929**, *30*, 467. (b) Teller, E. *J. Phys. Chem.* **1937**, *41*, 109. (c) Herzberg, G.; Longuett-Higgins, H. C. *Trans. Faraday Soc.* **1963**, *35*, 77. (d) Herzberg, G. *The Electronic Spectra of Polyatomic Molecules*; Van Nostrand: Princeton, 1966; pp 442. (e) Gerhartz, W.; Poshusta, R. D.; Michl, J. *J. Am. Chem. Soc.* **1977**, *99*, 4263. (f) Michl, J.; Bonacic-Koutecky, V. *Electronic Aspects of Organic Photochemistry*; Wiley: New York, 1990. (g) Bonacic-Koutecky, V.; Koutecky, J.; Michl, J. *Angew. Chem., Int. Ed. Engl.* **1987**, *26*, 70. (h) Mead, C. A.; Truhlar, D. G. *J. Chem. Phys.* **1979**, *70*, 2284. (i) Keating, S. P.; Mead, C. A. *J. Chem. Phys.* **1987**, *86*, 2152. (j) Tully, J. C.; Preston, R. K. *J. Chem. Phys.* **1987**, *55*, 562. (k) Blais, N. C.; Truhlar, D. G.; Mead, C. A. *J. Chem. Phys.* **1988**, *89*, 6204.

(36) (a) Bernardi, F.; De, S.; Olivucci, M.; Robb, M. A. *J. Am. Chem. Soc.* **1990**, *112*, 1737. (b) Bernardi, F.; Olivucci, M.; Robb, M. A. *Acc. Chem. Res.* **1990**, *23*, 405. (c) Bernardi, F.; Olivucci, M.; Ragazos, I. N.; Robb, M. A. *J. Am. Chem. Soc.* **1992**, *114*, 2752. (d) Bernardi, F.; Olivucci, M.; Robb, M. A.; Tonachini, G. *J. Am. Chem. Soc.* **1992**, *114*, 5805. (e) Bernardi, F.; Olivucci, M.; Ragazos, I. N.; Robb, M. A. *J. Am. Chem. Soc.* **1992**, *114*, 8211. (f) Palmer, I.; Bernardi, F.; Olivucci, M.; Robb, M. A. *J. Org. Chem.* **1992**, *57*, 5081. (g) Olivucci, M.; Ragazos, I. N.; Bernardi, F.; Robb, M. A. *J. Am. Chem. Soc.* **1992**, *114*, 8211. (h) Reguero, M.; Bernardi, F.; Jones, H.; Olivucci, M.; Robb, M. A. *J. Am. Chem. Soc.* **1993**, *115*, 2073. (i) Olivucci, M.; Ragazos, I. N.; Bernardi, F.; Robb, M. A. *J. Am. Chem. Soc.* **1993**, *115*, 3710. (j) Bernardi, F.; Olivucci, M.; Robb, M. A. *Isr. J. Chem.* **1993**, *33*, 256. (k) Olivucci, M.; Bernardi, F.; Ragazos, I.; Robb, M. A. *J. Am. Chem. Soc.* **1994**, *116*, 1077.

(37) (a) Matos, J. M. O.; Roos, B. O.; Malmqvist, P. Å. *J. Chem. Phys.* **1987**, *86*, 1458. (b) Roos, B. O.; Andersson, K.; Fülscher, M. P. *Chem. Phys. Lett.* **1992**, *192*, 5.

(38) McWeeny, R.; Sutcliffe, B. T. *Methods of Molecular Quantum Mechanics*, 1st ed.; Academic Press: New York, 1969.

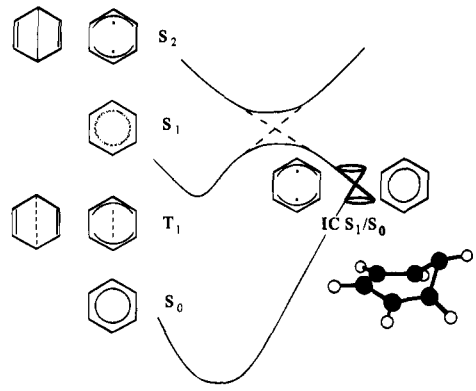

Figure 1. The origin of the S_0/S_1 surface crossing in benzene, showing diabatic correlations with spin couplings in the vertical excitation region.

spin couplings, we first review the situation for benzene itself to introduce some notation.

We have recently documented the S_0, S_1, and S_2 surfaces in benzene[20] and the T_1 surface has been studied by Osamura[39] and Van der Waals.[40] The topological features are summarized in Figure 1. The ground state is just the sum or superposition of the two Kekule structures, giving an aromatic structure. The equilibrium structure of S_1 benzene is an anti-aromatic structure (i.e. the difference of the two Kekule structures), which we indicate with a shaded circle. S_2 (ignoring the ionic and Rydberg states) is described by quinoid (Dewar type) and anti-quinoid spin couplings; we have previously characterized the quinoid equilibrium structure.[20] For T_1, Osamura has optimized both quinoid and anti-quinoid equilibrium structures, although they are only separated by a 1.4 kcal mol^{-1} barrier.

An overview of the results that we have obtained for styrene is presented in Figures 2 and 3 using the VB model. The diagrams are approximate because the coupling between ethylene and benzene groups is sometimes large, particularly in the triplet case. S_0 and S_1 correspond to the aromatic and anti-aromatic states of benzene in Figure 1. S_2 has a quinoid benzene ring, but note that this state is a combination of triplet quinoid benzene with triplet ethylene coupled to a singlet overall. The S_2 state of styrene is therefore not benzene-like. The S_3 state is ethylene-like (see Figure 3). It corresponds to a zwitterionic state of ethylene coupled to the aromatic state of benzene. The T_2 and T_1 states in the vertical excitation region correspond to triplet anti-quinoid benzene with triplet ethylene coupled to a triplet overall, and triplet quinoid benzene with singlet ethylene coupled to a triplet overall.

We now turn to the photochemical decay pathways. In benzene (Figure 1) the evolution along the S_1 relaxation path leads to decay via fast IC at a conical intersection point.[20] The electronic structure of the system at this point can be thought of as a real crossing between the quinoid (S_2) and aromatic (S_0) structures of benzene. The electronic structure of the S_1 surface changes character along the S_1 path due to an avoided crossing between S_1 and S_2 (dashed lines in Figure 1).

In Figure 2 we show the main points where the triplet and singlet manifolds cross in styrene and ISC is possible. S_1 styrene has two important S_1/T_2 intersection points: ISC_a and ISC_b. The first occurs after barrierless relaxation to the S_1 planar minimum where S_1 and T_2 are approximately degenerate. Here, the spin couplings on the benzene ring change from singlet anti-aromatic to triplet anti-quinoid. The second S_1/T_2 intersection point (ISC_b) occurs at a twisted S_1 minimum which is degenerate

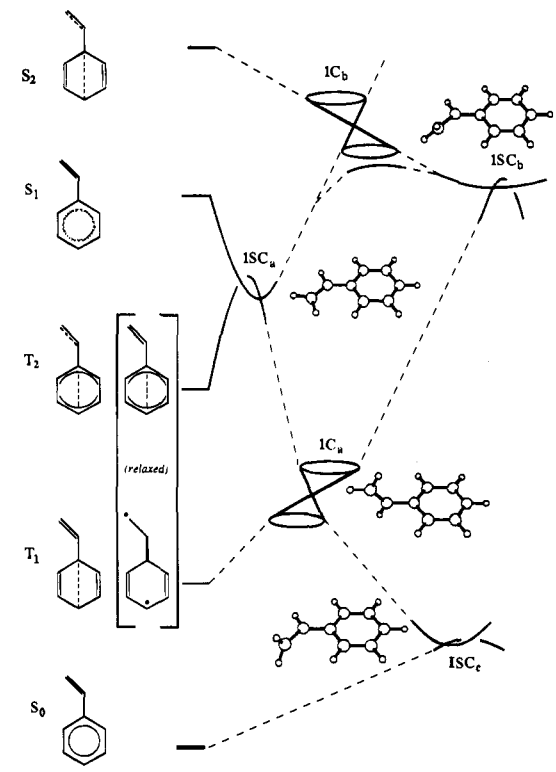

Figure 2. Origin of the singlet−triplet surface crossings in styrene, showing diabatic correlations with spin couplings in the vertical excitation region.

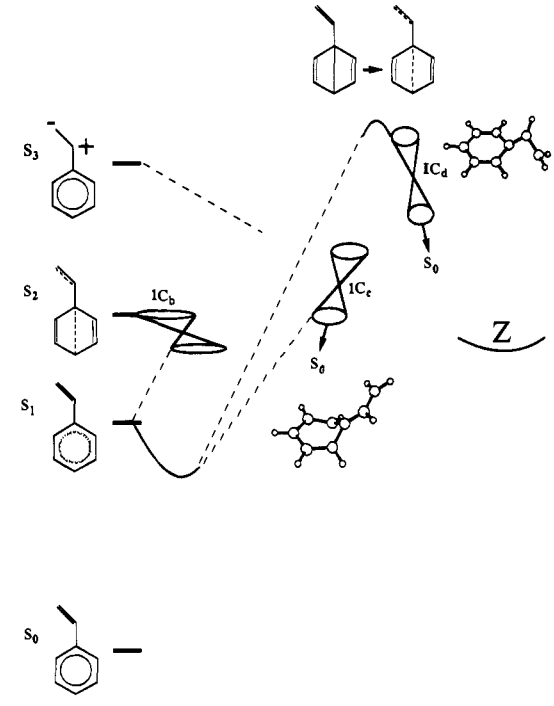

Figure 3. Origin of the singlet−singlet surface crossings in styrene, showing diabatic correlations with spin couplings in the vertical excitation region.

with T_2 and is reached after passage over a barrier associated with an avoided crossing between S_2 and S_1. The twisted S_1 minimum has a quinoid structure, correlates diabatically with S_2 in the vertical excitation region, and is triplet ethylene coupled to triplet benzene. The nature of the T_2 state at this geometry is similar except that the ethylenic fragment is singlet coupled. Thus the S_1/T_2 crossing at this twisted S_1 minimum simply corresponds to an inversion of spin in the ethylenic fragment.

(39) Osamura, Y. *Chem. Phys. Lett.* **1988**, *145*, 521.
(40) Buma, W. J.; van der Waals, J. H.; van Hemert, M. C. *J. Chem. Phys.* **1990**, *93*, 3733.

Table 1. CAS(8,8)/4-31G Planar Minima and Vertical Excitation Energies, Calculated Using Both 4-31G and 6-31G* Basis Sets

	geometry	energy/E_h	rel energy/ kcal mol^{-1} (4-31G)	energy/E_h	rel energy/ kcal mol^{-1} (6-31G*)	exptl 0−0/ kcal mol^{-1}
S_0	**a**	−307.2570	0.0	−307.6869	0.0	
T_1[a]	**d**	−307.1564	63.1	−307.5873	62.5	62.0[e]
vertical		−307.1355	76.3	−307.5653	76.4	
T_2	**e**	−307.1065	94.5	−307.5378	93.6	91.8[e]
vertical		−307.0947	101.9	−307.5251	101.6	
S_1	**b**	−307.0901	104.8	−307.5212	104.0	99.4[f]
vertical		−307.0812	110.4	−307.5119	109.9	
S_2[b]	**c**	−307.0563[c]	125.3	−307.4890[c]	124.2	112.5[g]
vertical		−307.0165	151.0	−307.4483	149.8	
ionic (vertical)		−	−	−307.4169[d]	169.5	

[a] T_1 twisted structure is lower in energy than T_1 planar (−307.1659). [b] Optimization constrained planar, as the twisted S_1/S_2 conical intersection is very close. [c] State averaged orbitals used, as the S_1 energy is −307.0637 (4−31G) or −307.4922 (6-31G*) at this geometry. [d] With the 6-31+G* basis, the S_2 covalent and ionic states are approximately degenerate. [e] Reference 25: 2.69 and 3.98 eV. [f] Reference 16: 4.31 eV. [g] References 2, 19, and 41: 4.88 eV.

A conical intersection (IC_a in Figure 2) between T_2 and T_1 provides a fully efficient route to T_1 and subsequent ISC at a T_1/S_0 crossing. At this conical intersection the spin coupling inverts in both fragments simultaneously while retaining overall triplet spin coupling. There are two T_1/S_0 crossing minima. One is shown in Figure 2 as ISC_c and corresponds to the twisted T_1 global minimum. At this crossing one simply has the spin change from triplet ethylene to singlet ethylene. The other T_1/S_0 crossing minimum (not shown) is virtually identical to the corresponding crossing that occurs in benzene.[32b] Thus the T_1/S_0 intersections are very similar to crossings that occur in ethylene or benzene.

In Figure 3 we illustrate the two structurally distinct conical intersections that occur in the singlet manifold and provide fully efficient IC pathways. A benzene-like conical intersection (IC_c) exists and arises in the same way as in benzene itself. Decay via this conical intersection would regenerate the starting product since the ethylene fragment is not involved. A different conical intersection IC_d occurs when both the ethylene−benzene torsional angle approaches 90° and there is a large (almost 90°) ethylene torsion. At this intersection point there is a simultaneous change in spin coupling in both the ethylenic and benzene fragments. If styrene is photoexcited to S_2 rather than to S_1, conical intersections between S_2 and S_1 become important.

(ii) **Mechanistic "Anchor Points": The Vertical Excitation Energies and Relaxed *Planar* Excited State Structures.** Our purpose in this section is to present the results of CASSCF calculations for the styrene singlet and triplet states—vertical and relaxed—which provide the "anchor" points for the mechanistic discussion to follow. In some cases these can be compared with spectroscopic results, to calibrate errors in our energetics.

Table 1 shows firstly that the relative energies calculated using the 4-31G and 6-31G* basis sets are almost the same. Compared to experiment, the S_0-S_1 0−0 excitation energy is overestimated by 5 kcal mol^{-1}, the T_1 0−0 energy reproduced to within 1 kcal mol^{-1}, and the T_2 energy overestimated by approximately 2 kcal mol^{-1}. (These errors are similar to those obtained by Roos[37a] for the corresponding benzene states.)

Hemley et al. obtained a value of 4.88 eV (112.5 kcal mol^{-1}) for the S_0-S_2 0−0 excitation[41] in a cooled jet experiment. Our value (Table 1) is about 12 kcal mol^{-1} above this. However, Swiderek,[25] Ziegler and Varotsis,[21] and Hemley[19,22,41] all find two states superimposed on each other in this region, one of which is ionic. Using the 6-31G* basis, we find a methyl$^-$benzyl$^+$ ionic state (labeled S_3) 169.5 kcal mol^{-1} above S_0 in the Franck−Condon region, and about 20 kcal mol^{-1} above S_2. With the diffuse 6-31+G* basis, S_2 and the ionic state are approximately degenerate, and a better treatment of dynamic correlation would probably lower the ionic state below S_2. Because this ordering has not been decided from experiment yet, we chose to compare the broad band maximum of 5.1 eV (118 kcal mol^{-1}) given by Swiderek with our S_2 vertical excitation energy. We overestimate this by about 30 kcal mol^{-1}, and can therefore expect 10−30 kcal mol^{-1} errors in the energies of the S_2 quinoid-like structures we calculate. These errors arise mainly from dynamic electron correlation effects associated with correlation of active (π)−inactive (σ) electrons; they will affect the barrier heights that we have calculated, but not the existence (or otherwise) of the minima and intersections characterized below.

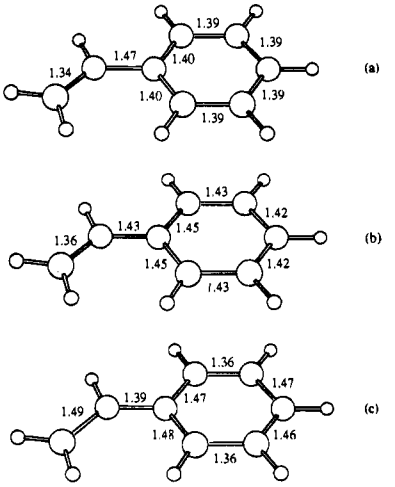

Figure 4. Relaxed planar singlet structures: S_0 (**a**, top), S_1 (**b**, middle), and S_2 (**c**, bottom). Energies in Table 1.

The structures of the S_0 and S_1 minima, shown in Figure 4 (**a** and **b**), are very similar to those of the corresponding states of benzene calculated at the same level of theory.[20] The major $S_0 \rightarrow S_1$ geometric distortions are ring expansion, a small increase in the ethylene bond length (1.34 Å → 1.36 Å), and a small contraction of the ethylene-benzene bond (1.47 Å → 1.43 Å). These changes have been established spectroscopically.[15,16] The energy of the S_1 structure changes by only 6 kcal mol^{-1} on relaxation (Malrieu[3] found 5 kcal mol^{-1}), implying that there will be little vibrational energy available to overcome barriers to further reaction. This is supported by a sharp structure seen in the fluorescence spectrum,[16] which persists even with a vibrational excess of 1200 cm^{-1}. Both S_0 and S_1 4-31G geometries were unchanged when optimizing with the 6-31G* basis.

(41) Leopold, D. G.; Hemley, R. J.; Vaida, V.; Roebber, J. L. *J. Chem. Phys.* **1981**, *75*, 4758.

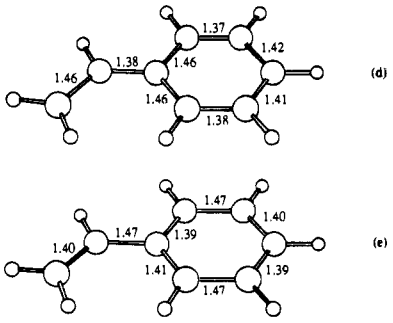

Figure 5. Relaxed planar triplet structures: T_1 (**d**, top), and T_2 (**e**, bottom). Energies in Table 1.

The relaxed S_2, T_1, and T_2 states were first optimized under planar constraint, because the 0−0 bands in the spectrum are thought to correspond to planar geometries.[21,25] All three states are quinoid/anti-quinoid in nature. In the benzene case, the S_2 surface is very flat indeed and there are quinoid/anti-quinoid and boat, chair, and half-chair structures within a very narrow energy band.[20] The planar styrene S_2 geometry is shown in Figure 4 (**c**). Note that the ethylene bond is now effectively a single bond (1.49 Å) and consequently free to twist. The geometries of T_1 and T_2 obtained under planar constraint are shown in Figure 5 (**d** and **e**). The T_1 state is quinoid, like S_2, with a long ethylene bond (1.46 Å) but a short ethylene−benzene bond (1.38 Å). This agrees with the suggestion of Swiderek[25] that the styrene T_1 state has butadiene-like character, with vibronic structure arising from the inversion of these two bond lengths. T_2 is anti-quinoid, with an ethylene bond of 1.40 Å and an ethylene−benzene bond of the same length (1.47 Å) as at the S_0 minimum.

The driving force for behavior of these states is now easily rationalized with the VB model we have described in the previous section. Consider the change in energy of the S_1 and S_2 states as the external methylene group is twisted. The energy of the S_1 state (singlet ethylene + anti-aromatic benzene) will increase dramatically, as this will involve breaking a double bond. The S_2 state (triplet ethylene + triplet quinoid benzene) will be stabilized because of the twisted ethylenic triplet equilibrium conformation). Along this coordinate, we expect the states to cross, so that at the fully twisted geometry the S_2 state is lower in energy than S_1 as indicated in Figure 2. The T_2 minimum (singlet ethylene + triplet quinoid benzene) will be destabilized by ethylenic double bond rotation and the twisted geometry will be a maximum, whereas T_1 will have an optimum geometry for the twisted structure.

(iii) **The Low-Temperature Isomerization Mechanism.** The experiments of Lewis and Bassani[8] have suggested two different ethylene isomerization mechanisms in styrene: one temperature independent and one temperature dependent. They suggest that a triplet state may be involved in the temperature-indepedent mechanism. Our objective in this subsection is to document the surface crossings that may lie on the temperature-independent path.

We begin our discussion with the S_1/T_2 crossing (ISC_a Figure 2) that occurs in the region of the S_1 planar minimum. Remarkably, the T_2 state lies only 4.8 kcal mol^{-1} below S_1 at this geometry (Table 2). Since the gradient of S_1 is zero at this geometry and the energy difference is very small, this point is effectively a critical point on the $(n-1)$-dimensional S_1/T_2 crossing surface. The gradient difference vector $\boldsymbol{x}_2$ (effectively the gradient on T_2 since the S_1 gradient is zero) is shown in Figure 6 and has components in both anti-quinoid ring expansion and ethylenic stretch. This is consistent with the geometries in Figures 4 (**b**) and 5 (**e**) and the qualitative VB picture given in Figure 2, in that $\boldsymbol{x}_2$ points toward the T_2 minimum.

The spin−orbit coupling constant computed at ISC_a was computed to be <1 cm^{-1} and thus the crossing is inefficient despite the small energy difference. This is consistent with the experimental observation that, for instance, in *trans*-1-phenylpropene the overall isomerization rate is constant at temperatures below 290 K—ISC_a is a temperature-insensitive bottleneck. A slow ISC rate is also consistent with the nanosecond lifetime and fluorescence quantum yield measured for both *trans*-1-phenylpropene (11.8 ns and 0.3 in ref 8) and styrene itself (14.6 ns and 0.24 in ref 12).

After ISC to T_2, fully efficient IC to T_1 can take place at the T_2/T_1 conical intersection labeled IC_a in Figure 2. This lies 10.4 kcal mol^{-1} below the relaxed S_1 planar minimum (ISC_a) and is almost degenerate with the T_2 minimum. Figure 7 (**g**) shows that, at this geometry, the ethylenic fragment is planar but there is almost 90° twist around the ethylene−benzene bond. However, because this ethylene−benzene bond is single, there will be no barrier to rotation from the planar T_2 minimum to the twisted T_2/T_1 intersection. As discussed previously, this crossing corresponds to the change from singlet ethylene + triplet quinoid benzene to triplet ethylene + singlet quinoid benzene. An unusual feature of this intersection is that the $\boldsymbol{x}_1$ and $\boldsymbol{x}_2$ directions defining the branching space are parallel, and hence the branching space is not $n-2$ but effectively $n-1$ dimensional. The geometrical deformation $\boldsymbol{x}_2$ which lifts the degeneracy is shown in Figure 8 and involves elongation of the ethylene bond (associated with the change from singlet to triplet ethylene) and benzene ring expansion (change from singlet benzene to triplet anti-quinoid benzene). This process can be thought of as two simultaneous singlet−triplet crossing processes going through an $(n-1)$-dimensional crossing surface. Notice that there is almost no component of the methylene torsion or the ethylene−benzene torsion in $\boldsymbol{x}_2$. This means that the intersection space extends into all regions involving these motions—crossing may take place at geometries which are nearly planar, for example. The point we have optimized is simply the lowest point on this line of intersection, but IC may occur at any geometry within the intersection space, depending on the dynamics of the $ISC_a \rightarrow IC_a$ relaxation.

The last stage in the relaxation mechanism starting at ISC_a involves decay from T_1 to S_0. We found (in agreement with previous work[26,35d,42,46]) that the lowest point on the T_1/S_0 crossing is coincident with the T_1 twisted geometry shown in Figure 7 (**h**) and labeled ISC_c in Figure 2. This structure has been experimentally detected by Bonneau using nanosecond laser flash photolysis[43] and Caldwell using time-resolved photoacoustic calorimetry.[44] The spin−orbit coupling constant at this geometry is again <1 cm^{-1}, and decay is therefore expected to be very slow compared to the fast IC at the T_2/T_1 intersection. However, the ISC at ISC_c must be fast enough to be consistent with the observed isomerization rate. Bonneau[43] gives the T_1 lifetime a value of 24 ns, and Caldwell[44] gives

(42) Bonneau, R.; Herran, B. *Laser Chem.* **1984**, *4*, 151.
(43) Bonneau, R. *J. Photochem.* **1979**, *10*, 439.
(44) (a) Caldwell, R. A.; Jacobs, L. D.; Furlani, T. R.; Nalley, E. A.; Laboy, J. *J. Am. Chem. Soc.* **1992**, *114*, 1623. (b) Caldwell, R. A.; Carlacci, L.; Doubleday, C. E.; Furlani, T. R.; King, H. F.; McIver, J. W. *J. Am. Chem. Soc.* **1988**, *110*, 6901. (c) Goodman, J. L.; Peters, K. S.; Misawa, H.; Caldwell, R. A. *J. Am. Chem. Soc.* **1986**, *108*, 6803. (d) Caldwell, R. A.; Cao, C. V. *J. Am. Chem. Soc.* **1982**, *104*, 6174.
(45) Ohmine, I. *J. Chem. Phys.* **1985**, *83*, 2348.
(46) (a) Arai, T.; Tokumaru, K. *Chem. Rev.* **1993**, *93*, 23. (b) Segawa, K.; Takahashi, O.; Kikuchi, O.; Arai, T.; Tokumaru, K. *Bull. Chem. Soc. Jpn.* **1993**, *66*, 2754. (c) Arai, T.; Sakuragi, H.; Tokumaru, K. *Bull. Chem. Soc. Jpn.* **1982**, *55*, 2204.

Table 2. Optimized Crossing Energies (in hartrees) at CAS(8,8)/4-31G Geometries, Using 4-31G (Top Line in Each Row) and 6-31G* (Bottom Line in Each Row) (Relative Energy Is the Average of the Energies of the Two States Which Cross)

	crossing (Figures 2 and 3)	geometry	S_0	T_1	T_2	S_1	S_2	energy rel to S_0/ kcal mol^{-1}
T_1 twisted min.	ISC_c	**h**	−307.1670	−307.1659				56.8
			−307.5954	−307.5968				57.0
S_0/T_1	ISC_d	**j**	−307.0839	−307.0850				108.3
(benzene-like)			−307.5168	−307.5182				106.3
T_1/T_2	IC_a	**g**		−307.1084	−307.1069			93.7
				−307.5384	−307.5371			93.6
S_1 twisted min.	ISC_b	**f**			−307.0658	−307.0630		120.9
			−307.6177		−307.4977	−307.4957		119.4
S_1/S_2	IC_b	**i**				−307.0598	−307.0550	125.3
						−307.4922	−307.4885	123.4
S_0/S_1	IC_c	**m**	−307.0509			−307.0452		131.2
(benzene-like)			−307.4881			−307.4829		126.4
S_0/S_1	IC_d	**l**	−307.0277			−307.0204		146.2
			−307.4652			−307.4601		140.8
S_1 planar min.	ISC_a	**b**			−307.0977	−307.0901		102.4
					−307.5290	−307.5212		101.6
S_0 planar min.	−	**a**	−307.2570					0.0
			−307.6869					0.0

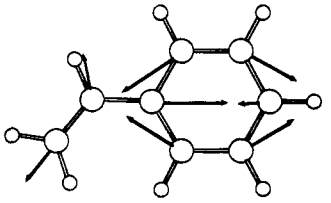

Figure 6. Gradient difference vector $\mathbf{x}_2$ at the S_1/T_2 planar crossing (ISC_a in Figure 2).

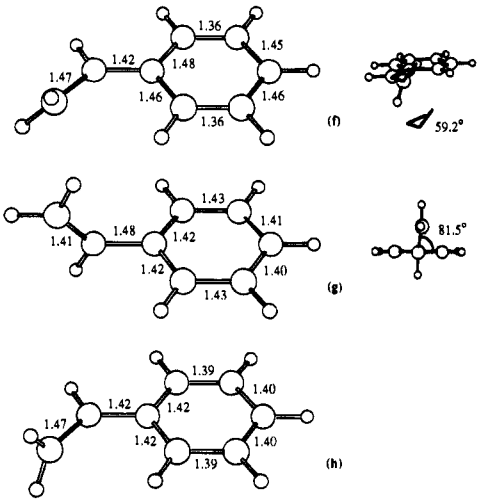

Figure 7. S_1 twisted minimum (**f**, top), T_1/T_2 intersection (**g**, middle), and T_1 twisted minimum (**h**, bottom). Energies in Table 2.

values in the range 20−100 ns. When compared with the singlet lifetimes measured for *trans*-1-phenylpropene and styrene (11.8 and 14.6 ns), the T_1 lifetime is longer. Thus the $T_1 \rightarrow S_0$ decay process appears to be slower than the $S_1 \rightarrow T_2$ decay and must therefore control the isomerization rate along this pathway (i.e., it must correspond to the overall bottleneck for the reaction). Calculations have shown that methylene pyramidalization and twisting motions increase the spin−orbit coupling,[44a,b] which suggests that vibration along these coordinates may promote decay.

The lack of observable phosphorescence from the T_2 state can be understood on the basis of our results. Once the decay to T_2 has taken place a barrierless twisting to IC_a leads to a femtosecond relaxation to T_1. Phosphorescence from T_2 would occur on a much longer time scale.

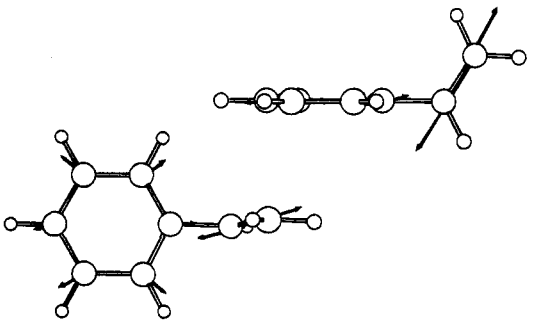

Figure 8. Direction of the gradient difference x_1 and derivative coupling x_2 vectors at the T_1/T_2 intersection (IC_a in Figure 2).

The lifetime (24 ns) and twisted structure of the T_1 minimum associated with ISC_c are consistent with the quantum yield for the triplet sensitized isomerization (0.5) which is independent of the energy of the sensitizers used. Energy redistribution should therefore take place, and decay at ISC_c should not be affected by the previous relaxation motion along S_1, T_2, and T_1. This suggests that 50% of the styrene which decayed from S_1 to T_2 via ISC_a should isomerize eventually at ISC_c. However, the measured quantum yield for fluorescence (0.24) and the derived quantum yield for ISC (0.4,[14] 0.6[8b]) are less than one, which suggests that there must be another decay step which does not lead to isomerization. One possibility for this decay involves an additional benzene-like[32b] T_1/S_0 crossing (spin−orbit coupling <1 cm^{-1} in benzene itself) that occurs some 12 kcal mol^{-1} higher than the T_1/T_2 conical intersection minimum (Table 2), almost degenerate with the S_1 vertical excitation (Table 1). This structure is shown in Figure 11. Because the ethylene double bond (1.34 Å) is unchanged in this region, no isomerization can occur, and any ISC at this geometry competing with decay at the twisted T_1 minimum will reduce the observed isomerization quantum yield.

(iv) Photochemical Isomerization at Higher Temperatures. Lewis and Bassani[8] suggest that this process, which begins to operate above room temperature in *trans*-1-phenylpropene, involves singlet states only. In this section we shall examine five mechanisms that could correspond to a decay process involving an excited state barrier.

We consider the accepted mechanism for *cis*−*trans* isomerization in aryl olefins first. This assumes that $S_1 \rightarrow S_0$ IC occurs at the minimum on S_1—where the double bond is twisted—which arises from an avoided crossing of the S_1 and S_2 states. Figure

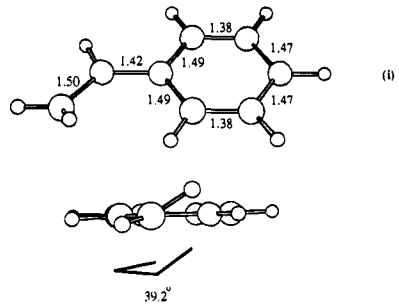

(i)

Figure 9. S_1/S_2 conical intersection geometry **i** (IC_b in Figures 2 and 3).

7 (**f**) shows that this minimum has a quinoid ring geometry like the S_2 minimum in Figure 4 (**c**), and that the terminal methylene is twisted by 60°. Because the energies of the S_1 and S_0 states differ by 76 kcal mol^{-1} at this geometry (Table 2), we would not expect IC to occur at this point. For this reason, the assumed mechanism seems very unlikely.

Table 2 shows that the S_1 twisted minimum lies 16 kcal mol^{-1} above the S_1 planar minimum. A frequency calculation (at a lower level of theory: STO-3G) suggests that this is a true minimum, but we have not been able to locate a transition structure along the reaction path between planar and twisted minima. There are two reasons for this. Firstly, the ethylene bond at the twisted minimum is single and free to rotate. This rotation is one of several low−frequency modes, suggesting that the twisted minimum is a broad and shallow well on the S_1 surface. The second reason is due to the S_1 and S_2 states being within several kilocalories per mole of each other in this region. The lowest energy point on a conical intersection between S_1 and S_2 (which is shown in Figure 9) differs from the S_1 twisted minimum only in the angle of twist (45°). The location of this intersection at 2 kcal mol^{-1} (Table 2) above the twisted minimum suggests that, lacking a well-defined transition structure, we can set an upper bound to the planar → twisted → planar barrier on S_1 at 16 + 2 = 18 kcal mol^{-1}. This agrees with previous calculations by Bendazzoli[5,6] and Malrieu,[3] while Rockley and Salisbury[28] have estimated a slightly lower value of 10−12 kcal mol^{-1} from experiment.

There are four alternative routes from S_1 to S_0 which are consistent with the surface crossings we have optimized: Path **1**, ISC from the twisted S_1 intermediate to T_2 (ISC_b); Path **2**, adiabatic isomerization on S_1 followed by ISC to T_2 at the planar S_1 minimum $(ISC)_a$; Path **3**, IC from the twisted zwitterionic S_1 intermediate (Z in Figure 3); and Path **4**, IC via the S_1/S_0 conical intersection IC_d.

Paths **1** and **2** involve the twisted S_1 minimum, but not as a point of IC. Table 2 shows that at this point, T_2 is only 2 kcal mol^{-1} lower in energy. This region of S_1 therefore provides a point of ISC to T_2 which we have indicated as ISC_b in Figure 2. The gradient difference vector $\mathbf{x_2}$ (the direction of motion that lifts the S_1/T_2 degeneracy) is shown in Figure 10. It corresponds to a terminal methylene twisting mode coupled with compression of the ethylene bond, combined with expansion of the ethylene−benzene bond and ring distortion from quinoid to anti-quinoid. Overall, this motion would lead to the anti-quinoid T_2 planar structure. Thus an initial ISC at ISC_b (followed by decay via the T_2/T_1 conical intersection described above) provides path **1** for the observed temperature-dependent isomerization of 1-phenylpropene. The barrier of <18 kcal mol^{-1} is now associated with the energy required to reach the ISC_b decay point.

The rate of ISC in the region of the S_1 twisted minimum (ISC_b) could well be higher than near the planar S_1 minimum

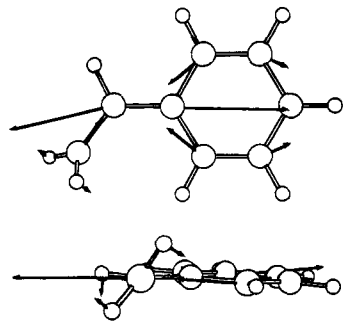

Figure 10. S_1/T_2 twisted crossing (ISC_b in Figure 2): two views of the gradient difference vector x_2.

Scheme 2

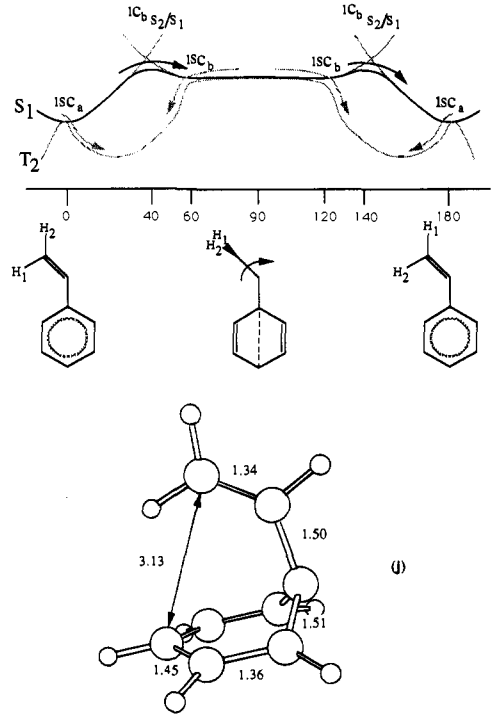

(j)

Figure 11. Geometry of the S_0/T_1 benzene-like intersection **j** (ISC_d).

(ISC_a). The spin−orbit coupling constant at ISC_b was computed to be <1 cm^{-1} (which follows from there being almost no change in orbital angular momentum associated with the change in spin) and the system must carry out many oscillations before ISC can occur. However, as illustrated in Scheme 2, the S_1 and T_2 states are degenerate over an almost flat region of the S_1 surface from 60° to 120° rotation. Furthermore, since this is effectively an adiabatic transition state for rotation, the motion will be slow and this will increase the probability of ISC.

Path **2**—adiabatic isomerization on S_1 followed by ISC to T_2 at the planar S_1 minimum (ISC_a)—may compete with path **1**. Both pathways involve the same thermal activation, but without explicitly considering the nuclear dynamics we can only guess at the branching ratio.

The observed temperature-dependent decay could also correspond to S_1 → S_0 IC (path **3**) via a twisted zwitterionic intermediate. Figure 12 shows that the structure of the zwitterionic S_1 minimum is very different from the twisted covalent minimum: the benzene aromatic ring is almost unchanged from S_0, but the ethylenic bond is stretched and the terminal methylene group is both twisted and highly pyramidalized. This intermediate is a simple closed shell species and correlates with S_3 in the vertical excitation region (Figure 3). The geometry was optimized at the SCF level and the energy

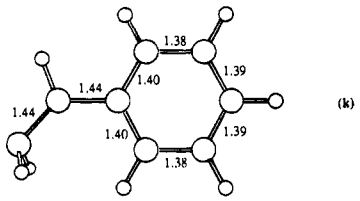

Figure 12. Geometry of the SCF ionic minimum **k**.

Table 3. Energies (in hartrees) of the S_0, S_1, and the Methyl$^-$ Benzene$^+$ Ionic States at Various Geometries Calculated Using the 6-31G* Basis

	geometry	S_0	S_1	ionic	ionic above S_0 (at this geometry)/ kcal mol^{-1}
ionic min.	**k**	−307.5598	−307.4446	−307.4871	45.6[a]
S_0 planar min.	**a**	−307.6869	−307.5119	−307.4169	169.5[b]
S_1 twisted min.	**f**	−307.6177	−307.4957	−307.4293	118.3[b]

[a] CI only, using closed shell SCF orbitals. [b] With the 6-31+G* basis, the S_2 covalent and ionic states are approximately degenerate.

recalculated using a CI (configuration interaction) computation in the 8 in 8 active space starting from the SCF π orbitals (Table 3). The zwitterionic minimum lies only 5 kcal mol^{-1} above the planar S_1 minimum and is therefore more stable than the twisted covalent S_1 minimum. Including dynamic electron correlation would lower the energy of the ionic minimum further. We did not determine the energy barrier of S_1 leading to the zwitterionic well since the ionic and S_0 states at this point are separated by 46 kcal mol^{-1}, and IC is therefore unlikely to occur. Only if initial hydrogen migration from the twisted methylene could efficiently lower the S_1-S_0 energy gap at this point (as suggested by Ohmine[45] for ethylene and butadiene) would the probability of decay increase. However, there is experimental evidence against the involvement of an ionic state in the isomerization mechanism: Lewis and Bassani[8b] suggest that analysis of the Arrhenius parameters does not support a polar transition state for singlet state isomerization.

Finally, we discuss path **4**: fully efficient decay via an S_0/S_1 conical intersection which leads to isomerization. We have located such an intersection (which corresponds to IC_d in Figure 3) at 39 kcal mol^{-1} above the planar S_1 minimum. Its structure is shown in Figure 13 (**L**): the benzene ring geometry is quinoid while the ethylenic bond is completely broken, and free to twist. Although the computed barrier of 39 kcal mol^{-1} is certainly an overestimate, this energy is too great for path **4** to be responsible for the temperature−dependent isomerization in styrene itself (even if we have overestimated by ~20 kcal mol^{-1}). Furthermore, path **4** may never operate because there is a lower energy IC channel (to be discussed in the next section) which does not lead to isomerization.

In summary, our results suggest that the triplet manifold is involved in the temperature-dependent mechanism. However, both path **1** and path **2** may be active. Since the spin−orbit coupling is very small in both cases, the velocity as the system traverses the crossing region must play a deciding role. The velocity in the region associated with ISC_b (twisted S_1 structure) must be very small since it is at the top of the barrier. In contrast, the velocity at ISC_a (planar S_1 minimum) will be large since it has the kinetic energy released after passage over the barrier. Because of this, we can argue that ISC_b should be more efficient than ISC_a. Decay along path **1** involves a change in the rate of isomerization with increasing temperature due to the switching from a slow (ISC_a) to a faster ISC process (ISC_b). This is certainly consistent with the increase in isomerization rate observed in both of the 1-phenylpropene isomers tested.[8]

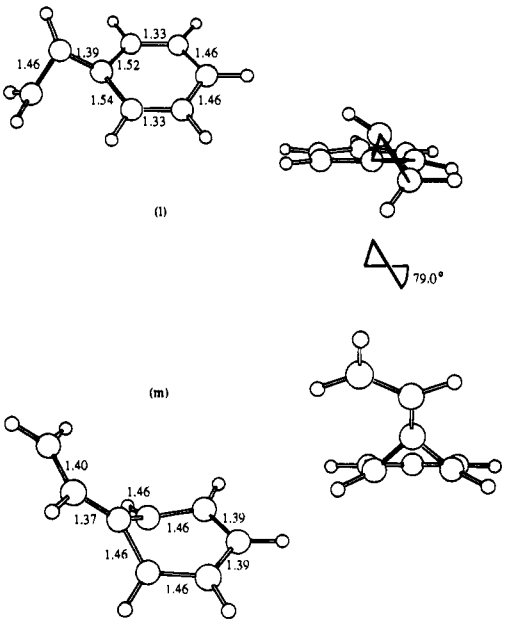

Figure 13. S_0/S_1 conical intersection structures: possible isomerization pathway IC_d (**l**, top) and benzene-like deactivation IC_c (**m**, bottom). Energies in Table 2.

A mechanism based upon adiabatic isomerization may still explain the experimental features if decay from T_2 is strongly polarized toward the reactant isomer, i.e. if the $S_1 \rightarrow T_2$ decay at the *trans* well yields primarily the *trans* isomer and *vice versa*. In this case the activation of an adiabatic isomerization process would indirectly cause a larger isomerization quantum yield for the reaction. This would be possible if the second benzene-like T_1/S_0 ISC decay channel was populated, although this appears to be too high in energy from our present calculations.

(v) Nonphotochemical Radiationless Relaxation Routes. Rockley and Salisbury[28] have demonstrated that the isomerization yield of 1-phenylpropene drops to zero as the excitation energy enters the S_2/S_3 band. This is consistent with fast IC from S_1 with an activation energy of ~3000 cm^{-1}, via a conical intersection where the ethylene torsion is restricted. For benzene, the activation energy required to enter the S_1 conical intersection regions is well-known to be 3000 cm^{-1} = 8 kcal mol^{-1} from spectroscopic work, and we have previously[20] computed a barrier of 23 kcal mol^{-1} for this process. We have optimized a benzene-like conical intersection in styrene, which lies 25 kcal mol^{-1} above the S_1 planar minimum. The geometry is given in Figure 13 (**m**) and shows that the benzene ring is virtually identical to that found at the benzene conical intersection itself. Because the ethylene double bond is only slightly stretched at this geometry, there is a barrier to ethylene twisting, and no isomerization can take place. This crossing may explain both the lack of photoisomerization on excitation to S_2 and the presence of a nonphotochemical decay channel at room temperature, assigned to IC by Lewis and Bassani.[8] Assuming that we overestimate the benzene-like intersection barrier in styrene by as much as we do, the benzene intersection itself, a channel 3-like IC mechanism (IC_c in Figure 3), must certainly provide one decay path for styrene. An 8 kcal mol^{-1} barrier on S_1 is accessible at 298 K, and whichever channel is responsible for the lower yield is already active in *trans*-1-phenylpropene at room temperature. A test of this hypothesis would be the observation of benzene-like photoproducts, although none have been detected to date.

Conclusions

Possible intersystem crossing (ISC) and internal conversion (IC) pathways have been studied by geometry optimization of the lowest energy crossing points and computation of the spin–orbit coupling constants. The optimized crossing points can be used to suggest several isomerization pathways in styrene. The low-temperature isomerization process observed by Lewis and Bassani would appear to be an ISC process involving the S_1/T_2 crossing in the immediate vicinity of the planar S_1 minimum. The existence of the lower-energy T_2/T_1 conical intersection explains the observed lack of phosphorescence. The temperature-dependent isomerization path cannot correspond to an $S_1 \rightarrow S_0$ IC decay as suggested by Lewis and Bassani but would appear to involve a second ISC with either $S_1 \rightarrow T_2$ decay at an S_1 twisted minimum or adiabatic isomerization on the S_1 state followed by ISC at the S_1 planar minimum. Finally, the involvement of the twisted S_1 zwitterionic intermediate in the isomerization process would appear to be unlikely since the quantum yields are not solvent dependent and the computed S_1/S_0 gap is too large to allow efficient IC. However, this may take place via the mechanism suggested by Ohmine.[45]

Acknowledgment. This research has been supported in part by the SERC (UK) under Grant Nos. GR/J25123 and GR/H58070. All computations were run on an IBM RS/6000 using a development version of the Gaussian program.[31]

Supporting Information Available: The Cartesian coordinates of styrene structures **a**–**m** in the figures (5 pages). This material is contained in many libraries on microfiche, immediately follows this article in the microfilm version of the journal, can be ordered from the ACS, and can be downloaded from the Internet; see any current masthead page for ordering information and Internet access instructions.

JA943621Z